

9-1-2008

The Power Flow Angle of Acoustic Waves in Thin Piezoelectric Plates

Iren E. Kuznetsova

Russian Academy of Sciences

Boris D. Zaitsev

Russian Academy of Sciences

Andrei A. Teplykh

Russian Academy of Sciences

Shrinivas Joshi

Marquette University, shrinivas.joshi@marquette.edu

Anastasia S. Kuznetsova

Saratov State University

The Power Flow Angle Of Acoustic Waves In Thin Piezoelectric Plates

Iren E. Kuznetsova

*Institute of Radio Engineering and Electronics of the Russian Academy of
Science, Saratov Branch,
Saratov, Russia*

Boris D. Zaitsev

*Institute of Radio Engineering and Electronics of the Russian Academy of
Science, Saratov Branch,
Saratov, Russia*

Andrei A. Teplykh

*Institute of Radio Engineering and Electronics of the Russian Academy of
Science, Saratov Branch,
Saratov, Russia*

Shrinivas G. Joshi

*Electrical and Computer Engineering Department,
Marquette University
Milwaukee, WI*

Anastasia S. Kuznetsova

*Saratov State University,
Saratov, Russia*

Abstract: The curves of slowness and power flow angle (PFA) of quasi-antisymmetric (A_0) and quasi-symmetric (S_0) Lamb waves as well as quasi-shear-horizontal (SH_0) acoustic waves in thin plates of lithium niobate and potassium niobate of X-, Y-, and Z-cuts for various propagation directions and the influence of electrical shorting of one plate surface on these curves and PFA have been theoretically investigated. It has been found that the group velocity of such waves does not coincide with the phase velocity for the most directions of propagation. It has been also shown that S_0 and SH_0 wave are characterized by record high values of PFA and its change due to electrical shorting of the plate surface in comparison with surface and bulk acoustic waves in the same material. The most interesting results have been verified by experiment. As a whole, the results obtained may be useful for development of various devices for signal processing, for example, electrically controlled acoustic switchers.

SECTION I.

Introduction

As is well known, the angle between propagation direction of wave and power flow (PFA) is a very important parameter for development of various acoustic devices.^{1,2} The values of this angle for different types of surface (SAW) and bulk (BAW) acoustic waves are presented in many papers.^{3,4} For bulk waves, one can use the surface of reversed velocities (the surface of slowness) for the analysis of this angle.⁵ In our paper, the line formed by the end of reversed velocity vector for plate and surface acoustic waves for various propagation directions is called the curve of slowness. This curve shows phase velocity anisotropy and the value of the angle between phase and group velocities. If the curve of slowness is a circle, the directions of phase and group velocities coincide, and PFA is equal to zero. It should be noted that today the great interest of researchers is attracted by acoustic waves in piezoelectric plates that are thin relative to the wavelength.^{6-7,8} It has been found that symmetric (S_0) and shear-horizontal (SH_0) waves are characterized by a higher value of the electromechanical coupling coefficient compared with SAW in the same material, and this allows using these waves for development of various high-sensitive sensors.^{6-7,8,9} Moreover, it has been shown that the characteristics of these waves strongly depend on electrical boundary conditions on the plate surface.^{10,11} Today, however, information on PFA and curves of slowness of plate acoustic waves is practically absent. The influence of electrical boundary conditions on PFA and the aforementioned curves was not studied. But such information is extremely interesting with the advent of crystals that possess a strong piezoeffect.^{12,13}

In this connection, we have carried out the theoretical analysis of PFA of antisymmetric (A_0) and symmetric (S_0) Lamb waves as well as shear-horizontal (SH_0) waves in thin plates of lithium niobate and potassium niobate for various propagation directions in the main crystallographic X, Y, and Z-cuts. The curves of the slowness of such waves on the aforementioned crystallographic cuts for various values of plate thickness were also constructed. We have investigated the influence of electrical shorting of one plate surface on the value of PFA and curve of the slowness. The most interesting obtained results have been verified by experiment.

SECTION II.

Theoretical Analysis of Curves of Slowness and PFA of A_0 , s_0 , and SH_0 Waves in Thin Piezoelectric Plates of $LiNbO_3$ and $KNbO_3$

The geometry of the problem under consideration is shown in Fig. 1. The wave propagates along the x_1 direction of a piezoelectric plate bounded by planes $x_3=0$ and $x_3=h$. The regions $x_3<0$ and $x_3>h$ correspond to vacuum. We consider a 2-D problem in which all field components are assumed to be constant in the x_2 direction. For the solution of the set problem, we used the standard motion equation, Laplace's equation, and constitutive equations for piezoelectric medium.^{1,2}

$$\begin{aligned}\frac{\rho \partial^2 U_i}{\partial t^2} &= \frac{\partial T_{ij}}{\partial x_j}, \\ \frac{\partial D_j}{\partial x_j} &= 0, \\ T_{ij} &= \frac{C_{ijkl} \partial U_l}{\partial x_k} + \frac{e_{kij} \partial \Phi}{\partial x_k}, \\ D_j &= -\frac{\varepsilon_{jk} \partial \Phi}{\partial x_k} + \frac{e_{jlk} \partial U_l}{\partial x_k}.\end{aligned}$$

(1)(2)(3)(4)

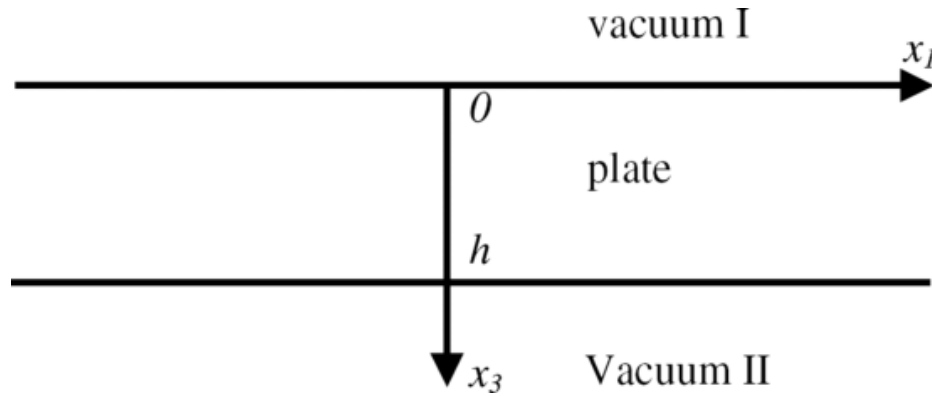


Fig. 1. The geometry of problem under consideration. Axis x_1 is wave propagation direction.

Here U_i is the component of mechanical displacement of particles, T_{ij} is the component of the mechanical stress, X_j is the coordinate, D_j is the component of the electrical displacement, Φ is the electrical potential, ρ is the density, t is the time, and C_{ijkl} , e_{ikl} , and ϵ_{jk} are the elastic, piezoelectric, and dielectric constants, respectively.

Outside the plate in regions I and II, the electrical displacement must satisfy the Laplace's equation:

$$\partial D_j^I / \partial x_j = 0, \partial D_j^{II} / \partial x_j = 0, \quad (5)$$

where $D_j^I = -\epsilon_0 \partial \Phi^I / \partial x_j$ and $D_j^{II} = -\epsilon_0 \partial \Phi^{II} / \partial x_j$. Here, ϵ_0 is the permittivity of vacuum, indices I and II denote that the values refer to regions $x_3 < 0$ and $x_3 > h$, respectively.

Acoustic waves propagating in the plate must also satisfy the mechanical and electrical boundary conditions. The mechanical stresses on both surfaces of the plate are absent and the mechanical boundary conditions take the form

$$T_{3j} = 0 \text{ at } x_3 = 0 \text{ and at } x_3 = h \quad (6)$$

As for the boundary electrical conditions there are 2 distinct cases.

1. The plate is electrically free at both sides. In this case, the electrical boundary conditions imply the continuity of normal components of electrical displacement D_3 and electrical potential Φ

$$\Phi = \Phi^I, D_3 = D_3^I, \text{ at } x_3 = 0;$$

$$\Phi = \Phi^{II}, D_3 = D_3^{II}, \text{ at } x_3 = h. \quad (7)$$

2. The plate is electrically open at plane $x_3=0$ and shorted at plane $x_3=h$, i.e., it is covered by a perfectly conducting layer, thin relative to the wavelength, having negligible mechanical loading. In this case the electrical boundary condition at $x_3=h$ is

$$\Phi=0. \quad (8)$$

The electrical boundary conditions at the plane $x_3=0$ are the same as in previous cases. Substituting the solution as the plane inhomogeneous wave in equation system (1) to (4) and (5) yields, in the end, one system of 8 ordinary differential equations for piezoelectric plates and 2 systems of 2 ordinary differential equations for vacuums in regions $x_3<0$ and $x_3>h$, respectively.^{2,8} At first, the phase velocity (V) is considered as the given parameter of these systems. This allows finding the eigenvalues and eigenvectors as the functions of phase velocity and writing the matrix of boundary conditions by using (6), (7) or (6), (8). The sought value of phase velocity is that value for which the determinant of this matrix is equal to zero.

As a result, the values of all mechanical and electrical variables were found in the plate and vacuum.

To construct the curves of slowness, one should calculate the dependence of reversed phase velocity on the current Euler angle. The curve of the slowness is the locus of the ends of the vectors of the reversed phase velocity (see Fig. 2). The reversed phase velocity vector ($1/v_{ph}$) coincides with radius-vector of the curve drawn from the origin O in accordance with the current Euler angle. This radius-vector determines the direction of the phase velocity or wave propagation. In its turn, the direction of the group velocity (reversed group velocity) is normal to the curve of slowness at the point of the intersection of this curve with the wave propagation direction. Therefore, the curve of the slowness allows us to find the PFA as the angle between directions of phase and group velocities. Two situations were studied in this paper: 1) the plate is electrically open and 2) one side of the plate is electrically shorted, i.e., it is covered with a thin conducting layer without mass loading.

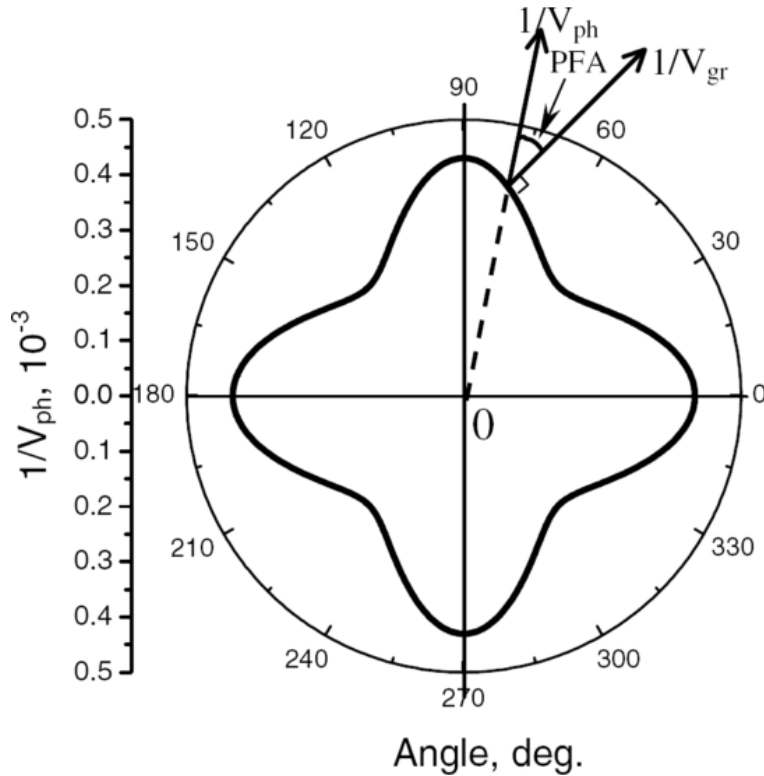


Fig. 2. The scheme for definition the directions of reversed phase and group velocities using the slowness curve.

The slowness curves of A_0 , S_0 , and SH_0 waves propagating in plates of lithium niobate and potassium niobate of all basic crystallographic X, Y, and Z cuts were constructed. The potassium niobate and lithium niobate material constants were taken from^{14,15} respectively. At analysis, 3 values of normalized thickness of piezoelectric plate were considered: $hf=500m/s, 1000m/s$, and $1500m/s$ (h =plate thickness, f =wave frequency). The most interesting results for (a) A_0 , (b) S_0 , and (c) SH_0 waves in lithium niobate and potassium niobate plates are presented on Fig. 3 and 4, respectively. Upper and lower rows correspond to the electrically open and electrically shorted plates.

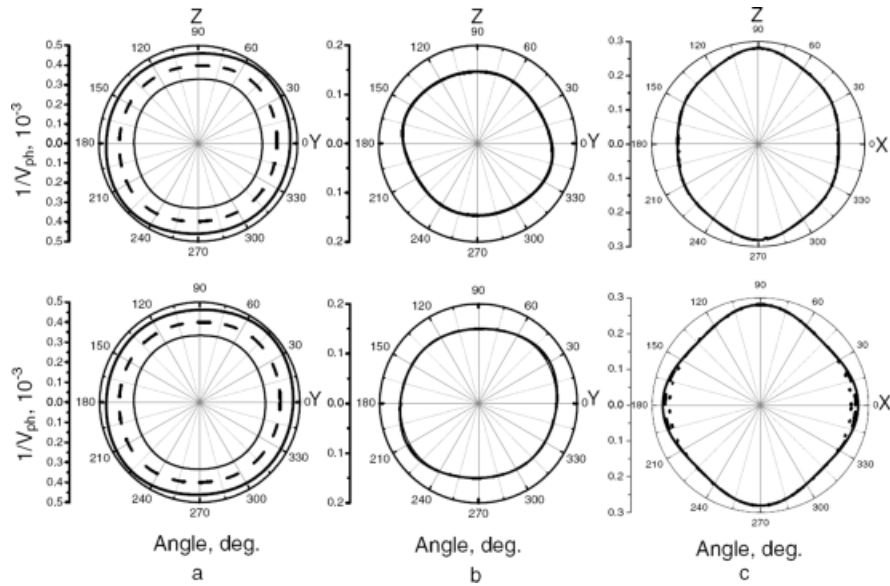


Fig. 3. The slowness curves of acoustic waves propagating in plates of lithium niobate: (a) A_0 in X cut, (b) S_0 in X cut, and (c) SH_0 in Y cut for different values of parameter hf : 500 m/s (solid line), 1000 m/s (dashed line), and 1500 m/s (thin solid line). Upper and lower rows correspond to electrically open and electrically shorted plates, respectively.

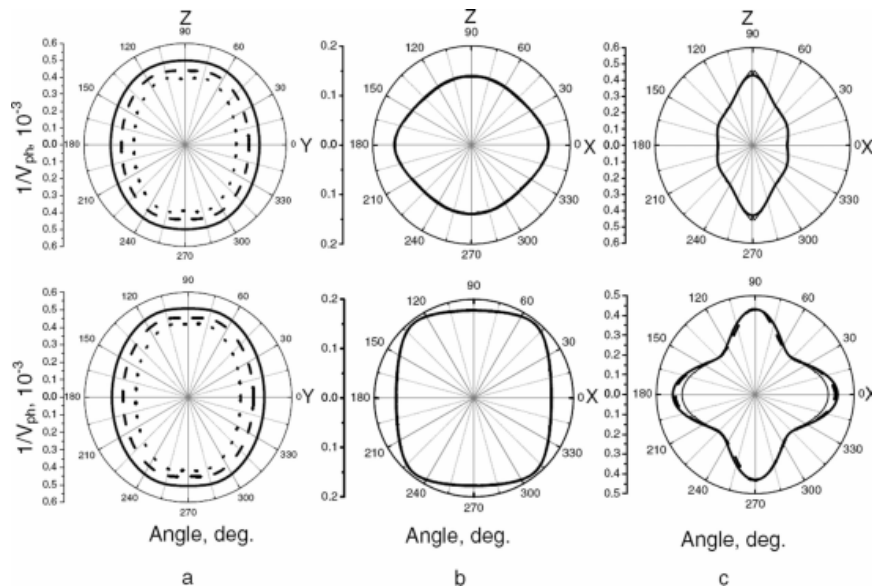


Fig. 4. The slowness curves of acoustic waves propagating in plates of potassium niobate: (a) A_0 in X cut, (b) S_0 in Y cut, and (c) SH_0 in Y cut for different values of parameter hf : 500 m/s (solid line), 1000 m/s (dashed line), and 1500 m/s (thin solid line). Upper and lower rows correspond to electrically open and electrically shorted plates, respectively.

It has been found that obtained curves of slowness are characterized by complicated shapes. For most propagation directions, the group velocity of these

waves does not coincide with the phase velocity, and PFA value may be very high (Fig. 3 and 4). From these figures, one can see that curves of slowness for A_0 waves in lithium niobate and potassium niobate for electrically open and electrically shorted plate surfaces are practically the same. This may be explained by weak electromechanical coupling of these waves. But due to their strong dispersion, the curves' slowness differs for different values of parameter hf . As for strongly piezo-active S_0 and SH_0 waves, Figs. 3(b) and 3(c) and Figs. 4(b) and 4(c) show that electrical shorting of the surface leads to the strong changes of the shape of the slowness curves. One can see also that for S_0 and SH_0 waves, the slowness curves do not depend on parameter hf , excluding the SH_0 wave propagating in an electrically shorted plate for both materials under study. For this case, there are propagation directions with reversed phase velocity strongly dependent on electrical boundary conditions. Aforementioned regularities for plate acoustic waves were observed for other cuts of lithium niobate and potassium niobate.

It should be noted that the value of PFA may be determined by the other method.^{1,2} As is well known, the power flow is defined by Poynting vector:^{1,2}

$$P_i = -\frac{1}{2} \operatorname{Re} \left\{ \int_0^h \left(\frac{T_{ij}^* \partial u_j}{\partial t} \right) dx_3 + \int_{-\infty}^{+\infty} \left(\frac{\Phi^* \partial D_i}{\partial t} \right) dx_3 \right\}. \quad (9)$$

Here * means the complex conjugation. It is apparent that the power flow cannot cross the boundaries of the plate, and component $P_3 \equiv 0$. Therefore, the PFA may be defined as

$$\text{PFA} = \arctan \left(\frac{P_2}{P_1} \right). \quad (10)$$

As a result of conducted calculations in accordance with (10), the dependencies of PFA for A_0 , S_0 , and SH_0 waves in electrically open and electrically shorted plates of lithium niobate and potassium niobate on propagation direction were obtained. As before, we considered the main crystallographic X, Y, and Z cuts of lithium niobate and potassium niobate for different values of parameter hf .

The analysis of these dependencies showed that the value of PFA significantly depends on plate orientation and propagation direction. This may be confirmed by Fig. 5 and 6 (upper row), which show the dependence of PFA of (a) A_0 , (b) S_0 , and (c) SH_0 waves in electrically open lithium niobate and potassium niobate plate of X- and Y-cut, respectively, on propagation direction at different values of parameter

hf . One can see that PFA may reach the significant values. For example, for $Y - X + 75^\circ$, $X - Y$, and $X - Y + 70^\circ$ propagation directions in lithium niobate plate PFA of SH_0 , S_0 and A_0 waves are equal to -14.7° , 9.5° , and -5.4° , respectively, at $hf=500$ m/s. As for the potassium niobate plate, the PFA of SH_0 , S_0 , and A_0 waves are equal to -48.0° , 15.4° , and -10.7° , respectively, at $hf=500$ m/s for $Y - X + 75^\circ$, $Y - X + 17^\circ$, and $X - Y + 45^\circ$ propagation directions. Thus, the SH_0 wave is characterized by record high values of PFA in comparison with SAW and BAW in lithium niobate and potassium niobate. It may be explained by the fact that, together with physical anisotropy of crystal, there exists so-called geometry anisotropy, which is typical for all layered media.¹⁶

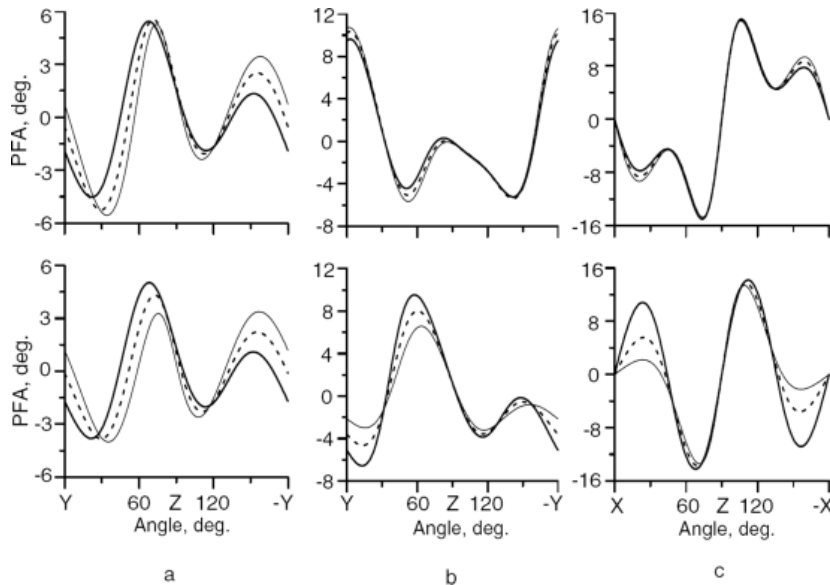


Fig. 5. PFA versus propagation direction for acoustic waves propagating in plates of lithium niobate: (a) A_0 in X cut, (b) S_0 in X cut, and (c) SH_0 in Y cut for different values of parameter hf . 500 m/s (solid line), 1000 m/s (dashed line), and 1500 m/s (thin solid line). Upper and lower rows correspond to electrically open and electrically shorted plates, respectively.

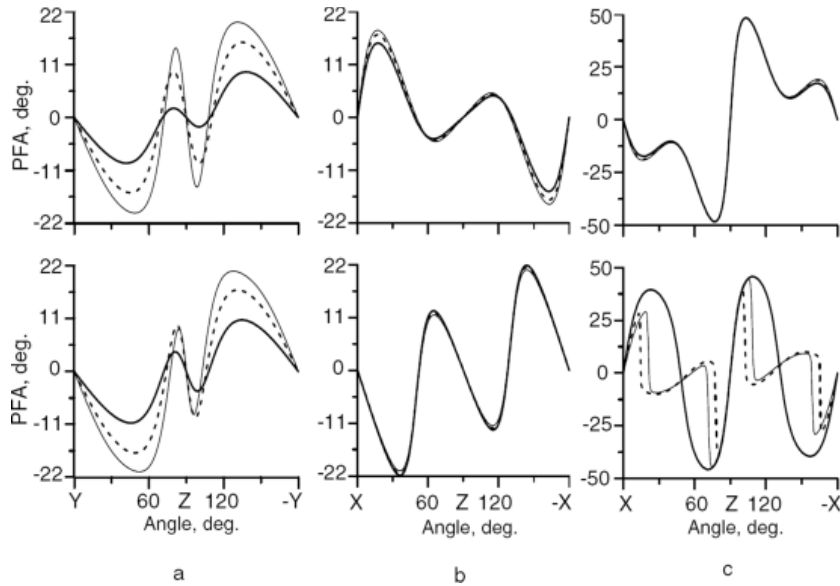


Fig. 6. PFA versus propagation direction for acoustic waves propagating in plates of potassium niobate: (a) A_0 in X cut, (b) S_0 in Y cut, and (c) SH_0 in Y cut for different values of parameter hf 500 m/s (solid line), 1000 m/s (dashed line), and 1500 m/s (thin solid line). Upper and lower rows correspond to electrically open and electrically shorted plates, respectively.

Fig. 5 and 6 (lower row) present the dependence of PFA of (a) A_0 , (b) S_0 , and (c) SH_0 waves in electrically shorted lithium niobate and potassium niobate plates of X- and Y-cut, respectively, on propagation direction at different values of parameter hf . The comparison of the upper and lower rows of Fig. 5 and 6 shows that the influence of electrical boundary conditions may be significant for S_0 and SH_0 waves. For example, for $Y - X + 150^\circ$ and $X - Y$ propagation directions, the change in PFA of SH_0 and S_0 waves may reach 21° and 15° , respectively, at $hf = 500$ m/s for lithium niobate plate. For potassium niobate plates, the values are equal to 56° and -32° for SH_0 and S_0 waves for $Y - X - 20^\circ$ and $Y - X + 152^\circ$ propagation directions, respectively. So the SH_0 wave is characterized by record high values of change in PFA in comparison with SAW in lithium niobate and potassium niobate due to higher level of electromechanical coupling. It can be also pointed out that electrical shorting of the plate surface may also change the sign of PFA. As for the A_0 wave, the change in PFA due to electrical shorting of the plate surface is insignificant.

SECTION III.

The Experimental Investigation of Electrical Shorting Influence on PFA of SH_0 Wave in Thin Piezoelectric Plates of Y-cut $LiNbO_3$

For experimental verification, we selected the SH_0 wave propagating along $X + 22^\circ$ -direction of Y-cut $LiNbO_3$ plate at $hf = 1000$ m/s. In this case, PFA is equal to 5.4° and -8.6° for electrically shorted and electrically open plates, respectively. For carrying out the experiment, we used the delay line with 3 interdigital transducers (IDTs) made on a 3-in. wafer of lithium niobate of Y-cut. This delay line is presented in Fig. 7. The wafer thickness was 0.5 mm. The input IDT launching acoustic wave was connected to a high-frequency generator; the output IDT₁ and IDT₂ receiving acoustic wave were connected to dual-beam oscilloscope. The output IDTs were set relative to the input IDT while keeping in mind the aforementioned values of PFA (Fig. 7). When one plate surface is electrically shorted, the acoustic beam should propagate through the channel 1 (input IDT-output IDT₁) and should be received only by IDT₁. When both plate surfaces are electrically open, the acoustic beam should propagate through the channel 2 (input IDT-output IDT₂;) and should be received only by IDT₂. The wave frequency and aperture were 1.93 MHz and 13 mm, respectively. The experiment was carried out in pulse operation with pulse duration $10 \mu s$.

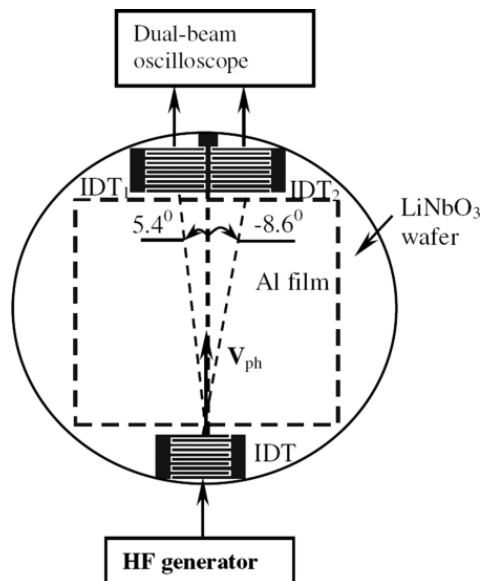


Fig. 7. Experimental setup.

On the first step, the experiment was carried out in the presence of thin aluminum film between input and output IDTs. The oscillogram of output signals from different channels is presented in Fig. 8(a). Upper and lower traces show the output signals from IDT₁ and IDT₂, respectively. One can see that the amplitude of signal from IDT₁ is 5 times more than one from IDT₂. It means that in this case channel 1 is operable.

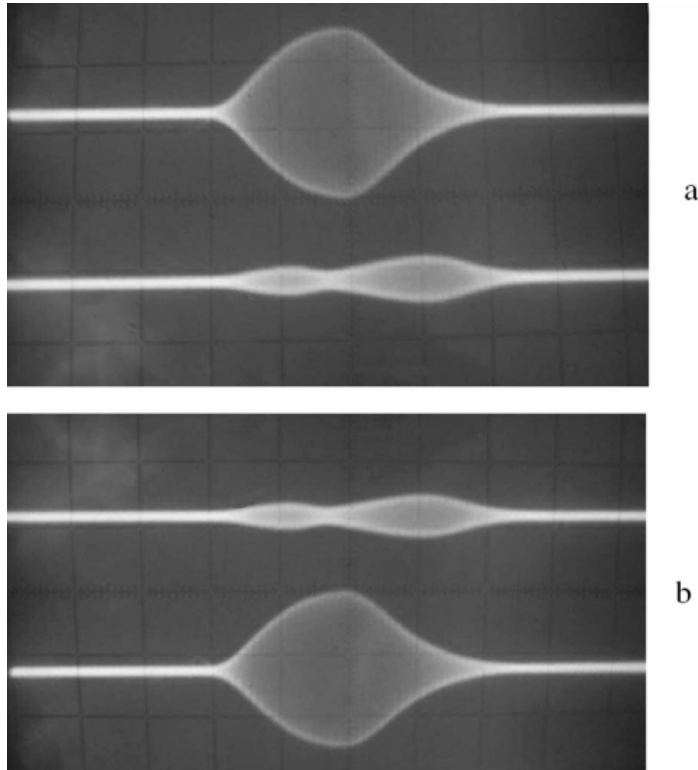


Fig. 8. Oscillograms of output signals: (a) in presence of thin Al film between IDTs, (b) in absence of thin Al film between IDT. Upper and lower traces show the output RF pulses from IDT₁ and IDT₂, respectively. Vertical scale: 4V/div, horizontal scale: 5 μ s/div.

On the second step, the aluminum film was removed by selective etching without any change of IDTs. Fig. 8(b) shows the corresponding oscillogram of output signals. One can see that in this case the channel 2 is operable. Thus, the experimental results are in good agreement with prediction based on theoretical data.

SECTION IV.

Conclusion

We have investigated the curves of slowness and power flow angle of A_0 and S_0 Lamb waves as well as SH_0 acoustic waves in thin plates of lithium niobate and potassium niobate for various cuts and propagation directions. As we have found, the obtained curves of slowness have a very complicated shape. For most propagation directions, the group velocity of these waves does not coincide with the phase velocity, and PFA value may be very large. It has been shown also that the electrical shorting of the plate surface leads to strong changes of slowness curves of the strongly piezo-active S_0 and SH_0 waves. Analysis has shown that there are the propagation directions, for which the electrical shorting leads to the appearance of the dependence of the reversed velocity on parameter hf . The conducted investigation has shown also that for certain crystallographic orientations of plate PFA of SH_0 and S_0 waves may reach significant values. For example, for $Y - X \pm 75^\circ$, $X - Y$, and $X - Y + 70^\circ$, propagation directions in lithium niobate plate PFA of SH_0 , S_0 and A_0 waves are equal to -14.7° , 9.5° , and -5.4° , respectively, at $hf=500$ m/s. As for the potassium niobate plate, the PFA of SH_0 , S_0 , and A_0 waves are equal to -48.0° , 15.4° , and -10.7° , respectively, at $hf=500$ m/s for $Y - X + 75^\circ$, $Y - X + 17^\circ$, and $X - Y + 45^\circ$ propagation directions. Moreover, the electrical shorting of the plate surface for certain crystallographic orientations of the plate may lead to significant change in PFA. For example, for $Y - X + 150^\circ$ and $X - Y$ propagation directions, the change in PFA of SH_0 and S_0 waves may reach 21° and 15° , respectively, at $hf=500$ m/s for the lithium niobate plate. For the potassium niobate plate, the aforementioned values are equal to 56° and -32° for SH_0 and S_0 waves for $Y - X + 20^\circ$ and $Y - X + 152^\circ$ propagation directions, respectively. Thus, the SH_0 wave is characterized by record high values of PFA in comparison with SAW and BAW in lithium niobate and potassium niobate. At that range, the electrical shorting changes not only the value of PFA but also its sign. The experimental results completely confirmed this theoretical conclusion.

As a whole, the results obtained may be useful for development of various devices for signal processing, for example, electrically controlled acoustic switchers. For this purpose, one can place between IDTs a semiconductor film with low voltage-controlled sheet conductivity.¹⁷

References

- ¹H. Matthews, *Surface Wave Filters: Design Construction and Use*, New York: John Wiley & Sons, 1977.
- ²*Acoustic Surface Waves*, Berlin: Springer-Verlag, 1978.
- ³A. J. Slobodnik, E. D. Conway, R. T. Delmonico, *Microwave Acoustics Handbook*, 1973.
- ⁴M. P. Cunha, D. Malocha, "Experimental and predicted SAW temperature behavior of langatate", *Proc. IEEE Ultrasonics Symp.*, pp. 245-248, 2000.
- ⁵R. D. Dieulesaint, *Elastic Waves in Solids: Applications to Signal Processing*, New York: John Wiley & Sons, 1980.
- ⁶I. E. Kuznetsova, B. D. Zaitsev, S. G. Joshi, I. A. Borodina, "Investigation of acoustic waves in thin plates of lithium niobate and lithium tantalate", *IEEE Trans. Ultrason. Ferroelectr. Freq. Control*, vol. 48, no. 1, pp. 322-328, 2001.
- ⁷M. Y. Dvoesherstov, V. I. Cherednik, A. P. Chirimanov, "Electroacoustic Lamb waves in piezoelectric plates", *Acoust. Phys.*, vol. 50, no. 5, pp. 512, 2004.
- ⁸S. G. Joshi, Y. Jin, *J. Appl. Phys.*, vol. 70, pp. 4113, Jun. 1991.
- ⁹I. E. Kuznetsova, B. D. Zaitsev, S. G. Joshi, I. A. Borodina, "Acoustic plate waves in potassium niobate single crystal", *Electron-Lett.*, vol. 34, no. 23, pp. 2280-2281, 1998.
- ¹⁰I. E. Kuznetsova, B. D. Zaitsev, S. G. Joshi, "SH acoustic waves in a lithium niobate plate and the effect of electrical boundary conditions on their properties", *Acoust. Phys.*, vol. 47, no. 3, pp. 282, 2001.
- ¹¹B. D. Zaitsev, I. E. Kuznetsova, S. G. Joshi, "Influence of electrical boundary conditions on structure of surface acoustic waves in potassium niobate", *Electron. Lett.*, vol. 35, no. 14, pp. 1205-1206, 1999.
- ¹²K. Yamanouchi, H. Odagawa, T. Kojima, T. Matsumura, "Theoretical and experimental study of super-high electromechanical coupling surface acoustic wave propagation in KNbO₃ single crystal", *Electron. Lett.*, vol. 33, no. 3, pp. 193-194, Jan. 1997.
- ¹³K. Nakamura, M. Oshiki, "Theoretical analysis of horizontal shear mode piezoelectric surface acoustic waves in potassium niobate", *Appl. Phys. Lett.*, vol. 71, no. 22, pp. 3203-3205, 1997.
- ¹⁴M. Zgonik, R. Schlessler, I. Biaggio, E. Voit, J. Tscherry, P. Gunter, "Materials constants of KNbO₃ relevant for electro- and acousto- optics", *J. Appl. Phys.*, vol. 74, no. 2, pp. 1287-1297, July 1993.
- ¹⁵G. Kovacs, M. Anhorn, H. E. Engan, G. Visintini, C. C. W. Ruppel, "Improved material constants for LiNbO₃ and LiTaO₃", *Proc. IEEE Ultrasonics Symp.*, vol. 1, pp. 435-438.
- ¹⁶L. M. Brekhovskikh, *Waves in Layered Media*, New York: Academic Press, 1980.
- ¹⁷M. Rotter, W. Ruile, G. Scholl, A. Wixforth, *IEEE Trans. Ultrason. Ferroelectr. Freq. Control*, vol. 47, no. 1, pp. 242, 2000.